Integrated Approach to Studying the Development and Final Network Properties of Urethane Acrylate Coatings

Susan M. Gasper, David N. Schissel, Linda S. Baker, Diane L. Smith, Randall E. Youngman, Lung-Ming Wu, Susan M. Sonner, Robert R. Hancock, Carrie L. Hogue, Steven R. Givens
Corning Incorporated
Corning NY USA

Introduction

Photopolymerization of acrylic materials to prepare crosslinked coatings is widespread.[1] Ease of preparation and versatility of properties have made these ideal materials for use in a wide variety of applications, including inks, adhesives, packaging materials and protective coatings for optical fibers. A complex interplay between chemical reactions and physical restraints takes place during the photopolymerization process. A fundamental understanding of the photocuring process is needed in order to avoid or minimize performance issues. This would facilitate some degree of control over the relationship between the chemical structure of coating components and final network structure of the crosslinked polymer, which dictates mechanical properties. For example, in the case of optical fiber, properties such as fiber durability and optical signal strength are highly dependent upon the properties of the coating materials.

Most commonly, the progress of photopolymerization reactions of acrylic materials has been followed by monitoring the disappearance of the reactive acrylic groups present in monomers and oligomers. Real time FTIR, as pioneered by Decker and co-workers,[2] has emerged as one of the most useful techniques for this purpose. The progress of these reactions has also been routinely studied by monitoring the heat of polymerization evolved using photo DSC.[3] In addition, extraction experiments have been used to monitor residual, unreacted acrylic materials that have not been incorporated into the developing polymer network.[4] Photocrosslinked systems have also been studied using methods that focus on the measurement of properties related to the development of crosslink density as the polymerization reaction proceeds. Commonly, dynamic mechanical analysis and Instron testing of stress-strain properties are done on fully polymerized systems.[1] Rheological monitoring of the development of viscoelastic properties in real time has been used to determine the point at which gelation occurs in photocrosslinked systems.[5] Solid state NMR relaxation measurements, in which the rate of ^{1}H bulk magnetization decay is related to the extent of crosslink density, have provided useful information regarding the network structure of polymeric materials.[6]

While the published studies on acrylate photopolymerizations using these different analytical approaches have provided many valuable insights into these systems, many of the studies have been limited to very simple systems – usually slower polymerizing methacrylate systems consisting of a single difunctional material along with a single photoinitiator. Also, very few photopolymerization studies employing UV curable urethane/acrylate oligomers, which are often used in performance coatings because of the wide range of desirable properties they can introduce, have been reported.[7] Consequently, the link between most of these systems and actual extremely fast polymerizing, high performance coatings (containing oligomeric components, additional monomers and additives – such as optical fiber coatings) has been somewhat limited.

To address this gap, polymer network development during photocuring was investigated in a series of model coatings more closely related to those of the very low modulus, urethane/acrylate coatings of practical interest.[8] These coatings are very fast polymerizing mixtures of high molecular weight urethane/acrylate oligomers and different acrylic co-monomers. By correlating kinetic measurements (real-time FTIR and UV rheology) with extraction studies and NMR relaxation measurements[9] conducted at various cure levels, and physical property testing of fully polymerized networks, we have attempted to develop a more comprehensive picture of network development as a function of component structure in these coatings.

Experimental Section
Materials
The poly(propylene glycol) materials (PPG2000 and PPG8000) were purchased from Bayer (Acclaim® 2200 and Acclaim® 8200), as was the Desmodur W® (4,4'-methylene bis(cyclohexyl-isocyanate), H12MDI). The 2-hydroxyethyl acrylate (HEA), dibutyltin dilaurate, and 2,6-di-tert-butyl-4-methylphenol (BHT) were purchased from Aldrich Chemical Co. The Photomer 4003 (ethoxylated (4) nonylphenol acrylate) and Photomer 8061 (propoxylated (3) methylether acrylate) were from Cognis. Irgacure 184 and 819 were from Ciba Specialty Chemicals. The polyols were heated at 40-50 °C for 12h under vacuum to remove traces of water prior to use. All of the other materials were used as received.

Oligomer Preparation
The oligomers were prepared from poly(propylene glycol), 4,4'-methylene bis(cyclohexyl-isocyanate) and hydroxyethyl acrylate using well known procedures.[10] In general, stoichiometric quantities of polyols, diisocyanate and hydroxyl functional acrylate were reacted together to give oligomeric mixtures having an average structure corresponding to that given in the text.

Formulation Preparation
The oligomer and co-monomers were mixed at 55 °C until thoroughly blended. Then the photoinitiator was mixed in until most of it had dissolved. The mixture was heated overnight in a 50-55 °C oven and then mixed again to form a homogeneous solution. Compositions were verified using HPLC and GPC. Viscosity measurements were obtained using a Brookfield CAP 2000L viscometer at 25 °C with a #4 spindle cone at a rate of 50 rpm.

Film Preparation and Photopolymerization Procedures
Wet films were cast on silicone release paper with the aid of a draw-down box having a 5 mil gap thickness. Fully polymerized films were prepared using a nitrogen purged Fusion Systems UV curing apparatus with a 600 watt/in D-bulb at 50% power and a belt speed of 10 ft/min. Partially polymerized films were prepared using a Fusion Systems UV curing apparatus with a 300 W/in D-bulb on a high speed, unpurged cure belt. Wet films cast on release paper were placed in a box with a fused silica window and purged with nitrogen. Exposure was controlled using an aluminum plate with a narrow slit beneath the face of the lamp in conjunction with a Kimwipe as a neutral density filter. Belt speed and neutral density filter thickness were adjusted to give the desired conversion level. Degrees of conversion were determined on a Bruker Vector FTIR spectrometer by monitoring the acrylate band (1406 cm^{-1}). Average conversion values were calculated from degrees of conversion determined for the top and bottom sides of the film at three locations along the length. The exposure received by the films in the cure box was measured with an IL390 light bug.

Real-Time FTIR

The rate of conversion of acrylate bands (1406 cm^{-1}) upon exposure to UV-vis radiation was monitored by FTIR on a Bruker IFS 66S spectrometer. Films with 1 mil thickness were drawn directly on a 3 bounce diamond coated ZnSe crystal in an ASI DuraSamplIR® accessory and purged with nitrogen for 1 minute. Films were exposed to UV irradiance from a Lesco Mark II spot cure unit conducted through a liquid light guide (~15-20 mW/cm^2 at 320-390 nm) while mid infrared spectra from 4000 cm^{-1} to 650 cm^{-1} were collected at 6 ms intervals. The reaction was monitored after a relatively short initial light pulse, after which the sample was exposed to a longer pulse to achieve maximum conversion. Composite conversion rate values were assigned as the slope of the linear portion of the conversion vs. time curve (10-40%).

UV Rheology

A Rheometric dynamic rheometer, RDA-II, was modified such that the sample between parallel plates with a 1 mil gap could be exposed to UV while its viscoelastic property was measured in real-time. A UV source (Green Spot) and a precision shutter system (Uniblitz VMM-T1) were used. The UV irradiance measured at the sample surface with an EIT SpotCure radiometer was 16 mW/cm^2. The reaction was monitored after a relatively short initial light pulse, after which the sample was exposed to a longer pulse to achieve maximum conversion. Electric signals, corresponding to rotational position and torque, were collected during irradiation and processed to give fundamental parameters of viscoelasticity, i.e., dynamic shear modulus, viscous modulus, elastic modulus, and damping factor (tan δ). Since the experiment is run at a single frequency, it is not possible to determine the gel point according to the Winter-Chambon criterion. Instead, an alternative definition (the attainment of a 45° phase angle (tan δ = 1) as the damping factor decreases) was used as an indicator of the critical gel point.[11]

Ultrasonic Extraction Procedure

Polymerized films were extracted three times, for 30 min, using methylene chloride and an ultrasonic extraction technique. Lower molecular weight components recovered in the extracts were characterized by reversed phase HPLC using a C18 column at 40 °C with an acetonitrile-water gradient and photodiode array detection. The oligomeric components were characterized by GPC at 40 °C using tetrahydrofuran as the eluent with refractive index detection. External standards were used for quantification of components while polystyrene standards were used to evaluate molecular weight distributions (Polymer Laboratories Easi-Cal PS-2 A and B standards plus PS-980 and PS-162).

NMR Measurements

^{1}H NMR data were collected using a commercial instrument and probes (Chemagnetics), in conjunction with a 4.7 T superconducting magnet. At this field strength, the resonance frequency for ^{1}H is 199.8 MHz. ^{1}H T$_2$ relaxation measurements were conducted using a Hahn echo pulse sequence to monitor the signal strength as a function of delay time between the π/2 and π pulses. All measurements in this study were made at room temperature on solvent swollen samples prepared by adding deuterated methylene chloride immediately before data acquisition. The ^{1}H Hahn echo data were evaluated by taking the height of the time domain echo in magnitude mode and subsequently plotting the normalized values as a function of delay time. In this manner, ^{1}H decay curves were generated using the bulk proton signal from each sample and therefore these data represent the characteristic properties of the entire sample. Numerical analysis of the ^{1}H decay curves was performed using the model of Kuhn *et al*.,[12] mathematically described by the relation

$$M(t) = A\exp\left\{\left(-\frac{t}{T_2}\right) - \left(\frac{qM_2 * t^2}{2}\right)\right\} + B\exp\left(-\frac{t}{T_2}\right) + C\exp\left(-\frac{t}{T_2^{sol}}\right)$$

(1)

where the prefactors A, B and C denote the fractional contributions from material having three distinct degrees of mobility; roughly corresponding to fully crosslinked chains, dangling chain ends and sol components, respectively. Although values for the two time constants, T_2 and T_2^{sol}, and the qM_2 parameter are also obtained, their interpretation is beyond the scope of this paper.

Mechanical Testing Procedures

Fully polymerized films were allowed to age (23 °C, 50% rh) for at least 16 hours prior to testing. Film samples were cut to a specified length and width (15 cm x 1.3 cm). Young's modulus, tensile strength at break, and elongation at break were measured using an Instron 5500 tensile tester. Glass transition temperatures of the fully polymerized films were determined by the tan δ curves measured on a Seiko-5600 DMS in tension at a frequency of 1Hz.

Results and Discussion

Two series of model coating formulations were studied in this work. These are summarized in Table 1 and structures of the oligomers and monomers used are shown in Table 2. In the first series, designated O1 to O3 (referred to as the O series), two urethane/acrylate oligomers were formulated at different oligomer/monomer weight ratios with the same co-monomer, Photomer 4003 (ethoxylated nonylphenol acrylate), to give coatings expected to have different crosslinking levels when fully reacted. In the second series, designated M1 to M3 (referred to as the M series), the oligomer 2xPPG2000 was formulated with different co-monomers at a 52/45 oligomer/monomer weight ratio to give coatings which should have similar crosslinking levels. In this series both Photomer 4003 and Photomer 8061 (propylene glycol monomethyl ether acrylate) were used as co-monomers, either individually or as a 50/50 mixture. In both sets of formulations the total photoinitiator level was set at 3% by weight, consisting of equal parts Irgacure 184 and Irgacure 819.

Table 1. Summary of formulations studied.

Sample	Formulation (oligomer//co-monomer)	Theor. g/mole of x-linking acrylate	Viscosity (Poise, 25°C)
O1	16 1xPPG2000//81 Ph4003	8460	6.3
O2	52 1xPPG2000//45 Ph4003	2650	56
O3	52 1xPPG8000//45 Ph4003	8420	151
M1	52 2xPPG2000//45 Ph4003	4830	90
M2	52 2xPPG2000//45 Ph8061	4830	17
M3	52 2xPPG2000//22.5 Ph4003/22.5 Ph8061	4830	34

The nature of the oligomer synthesis, as well as the polydisperse nature of the polyol reactants, ensures that the oligomers would consist of a mixture of materials having a distribution of molecular weight values.[13] Throughout our discussion we make the assumption that the various oligomers have a molecular weight equal to that of the ideal structure based on reactant stoichiometry described in the Experimental section (and as shown in Table 2). GPC measurements (data not shown) did confirm that the various oligomers had average molecular weights (relative to poly(styrene) standards) in the correct order (i.e. 1xPPG2000 < 2xPPG2000 < 1xPPG8000). Idealized crosslinking levels (in grams of material per mole of crosslink) were calculated by assuming that the only crosslinking points were the acrylic

end groups on the oligomers. The crosslinking levels are therefore determined by the amount and molecular weight of oligomer in a given formulation. The calculated crosslink density levels are also shown in Table 1.

Table 2. Structures of oligomers and co-monomers.

Material	Structure
1xPPG$_x$	HEA~H12MDI~PPG$_x$~H12MDI~HEA
2xPPG$_x$	HEA~H12MDI~PPG$_x$~H12MDI~PPG$_x$~H12MDI~HEA
Photomer 4003	
Photomer 8061	
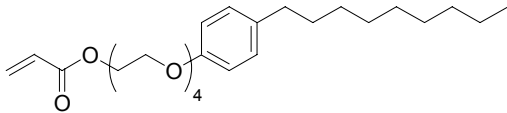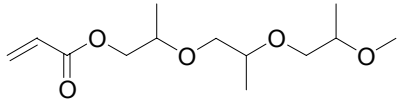
Because the materials examined in this study were extremely fast curing, we found it convenient to separate our study of the reaction into two parts. Kinetic measurement techniques were applied to the early stages of the curing reaction (0 to 40% conversion), roughly corresponding to reaction up to the gel point as determined by rheological measurements. Physical techniques to assess the structure of the developing polymer networks were applied at later stages of the reaction, from roughly 50% up to full conversion. The techniques included analysis of extracts from both partially and fully converted material, solid state NMR relaxation studies on partially and fully polymerized networks, and dynamic mechanical analysis and stress-strain property testing on fully polymerized materials. The lightly crosslinked nature of the materials, as well as their rapid curing rates, made it difficult to directly obtain and analyze samples with a degree of conversion less than 50%.

The kinetic data obtained for the early stages of the curing reactions are shown in Table 3 for both the O and M series of formulations. The relative conversion rates correspond to the slope in the time vs. acrylate concentration plot in the 10 to 40% conversion range as explained in the Experimental section. The gel time values were determined at the point at which storage and loss moduli became equal in the developing polymer network, and are expected to approximate the point at which a true, continuous load bearing network has been established.[6a] Also included in the table are the approximate degree of conversion values at the gel point. These were determined from separate FTIR and UV rheology experiments using the same sample thickness and radiation dose.

Table 3. Early stage reaction kinetic data and formulation acrylate concentrations.

Sample	Relative Conversion Rate	Gel Time, t_{gel} (sec)	DOC @ t_{gel} (%)	Relative [Acrylate] mole/g: total, x-linker, monomer
M1	65.48 ± 0.56	0.43 ± 0.02	26 ± 1	1.08, 0.18, 0.89
M2	40.48 ± 0.18	0.34 ± 0.05	14 ± 2	1.73, 0.18, 1.54
M3	51.23 ± 0.35	0.39 ± 0.04	20 ± 2	1.40, 0.18, 1.22
O1	69.19 ± 0.57	0.35 ± 0.01	22 ± 1	1.71, 0.10, 1.61
O2	82.37 ± 0.98	0.34 ± 0.01	21 ± 3	1.23, 0.34, 0.89
O3	61.43 ± 0.60	0.57 ± 0.04	30 ± 1	1.00, 0.11, 0.89

For the M series of formulations, in which the same oligomer and the same oligomer to monomer ratio were used, the relative conversion rate increased as the rate of physical property

development decreased (as indicated by an increase in t_{gel}). The fact that acrylate conversion is fast for M1 but network build-up is slow suggests that both reactive end groups of the crosslinking oligomer are not being incorporated efficiently at the early stages of the polymerization. For the M2 formulation, acrylate conversion is slow but network build-up appears to be very efficient as indicated by the short t_{gel}. This would suggest that in M2 both reactive end groups of the crosslinking oligomer are being incorporated efficiently in the early stages of the polymerization. The low initial viscosity of M2 (Table 1) may allow the large growing polymer chain radicals to remain more mobile in the early stages of the reaction, which in turn allows them to more readily couple and form a crosslinked network. M1 has a higher initial viscosity, which could result in earlier diffusion limited termination.[14] This would increase the rate of acrylate conversion (autoacceleration) but reduce the rate of large polymer chain radical coupling, resulting in an increase in t_{gel}.

The delayed gel point for M1 indicates that incorporation of both reactive end groups of the crosslinking oligomer is inefficient and suggests that the rapid acrylate conversion observed in this formulation must be dominated by the polymerization of the co-monomer. One potential explanation for the fast acrylate conversion but slow network formation in M1 could be a greater tendency of the co-monomer to self-associate and segregate itself from the oligomer. Surfactant-like association of Photomer 4003 to minimize interaction of hydrophobic alkylphenyl chains with the more hydrophilic polyether chains, both in the Photomer 4003 itself as well as in the oligomer, would increase the local concentration of acrylate groups associated with the co-monomer, thus leading to an increase in their polymerization rate. Enhanced polymerization rates attributed to hydrogen bonding which brings reactive acrylate groups into proximity have been suggested in other photocured systems.[15] The greater tendency of the Photomer 4003 acrylate groups to react with each other instead of the acrylate end groups in the oligomer would result in delayed gelation. The measured conversion rates reflect the amount of Photomer 4003 in the formulations, decreasing in the order M1 (all Photomer 4003) > M3 (mix of the two monomers) > M2 (all Photomer 8061). The trend in both t_{gel} values and degree of conversion measured at the gel point (M1 > M3 > M2) reflects delayed gelation with increasing amounts of Photomer 4003. Because the fast conversion of the Photomer 4003 dominates the early stages of the reaction, the total molar amount of acrylate present in each formulation, as well as the molar amount of acrylate coming from monomer (shown in Table 3), which both follow the order M2 > M3 > M1, does not appear to be important in this series.

For the O series formulations, the rate of acrylate conversion and the development of physical properties show a more direct relationship. The trend in the rate of acrylate conversion (O2 > O1 > O3) appears to be influenced by both initial viscosity and acrylate concentration. Although O1 has the highest level of acrylate, the rate of acrylate conversion is higher for O2, while the development of physical properties (indicated by t_{gel}) is nearly identical for the two formulations. The exceptionally low initial viscosity of O1 may delay the onset of autoacceleration relative to O2, leading to a lower overall acrylate conversion rate in the former. However, the initial low viscosity of O1 seems to facilitate the efficient incorporation of crosslinking oligomer into the network as suggested by t_{gel} and the degree of conversion at t_{gel} being equivalent to that for O2, in spite of a lower level of crosslinking acrylate in O1. In O2, a desirable balance of acrylate concentration and initial viscosity has been achieved to give a fast curing formulation. While the O3 formulation has the highest initial viscosity, it also has the lowest level of total acrylate concentration. The latter appears to control curing behavior in this formulation, as it exhibits the slowest conversion rate, the longest t_{gel} and the highest conversion level at t_{gel}.

Another useful comparison is between O2, M1 and O3. These formulations have the same oligomer/monomer weight ratio, the same co-monomer (Photomer 4003) and the molecular weight of

the oligomer increases going from O2 (1xPPG2000) to M1 (2xPPG2000) to O3 (1xPPG8000). In this series the observed trends in both conversion rate (O2 > M1 > O3) and t_{gel} and degree of conversion at t_{gel} (O2 < M1 < O3) appear to be controlled more by acrylate concentration than by the initial formulation viscosity. These trends are in fact opposite to what would be expected if increased initial coating formulation viscosity (O3 > M1 > O2) were to result in an earlier onset of autoacceleration. Increased acrylate conversion rate, shorter t_{gel} and a lower degree of conversion at t_{gel} are seen in coatings having both the larger total acrylate concentration and the greater concentration of crosslinking acrylate groups from oligomer, indicating the more dominant role played by these factors.

The second set of experiments, involving analysis of extracts from partially polymerized coatings and solid state NMR relaxation measurements on the partially developed polymer networks, were done on samples with a degree of conversion ranging from approximately 50% to full conversion. The molar percentages of monomers recovered from the various formulations as a function of degree of conversion are shown in Figure 1. Although measurements of recovered, soluble oligomeric material were also made, shifts in the molecular weight distribution in this material in some samples compared to the starting oligomer introduced uncertainties into the quantitation. As a result, conclusions were not drawn using this data.
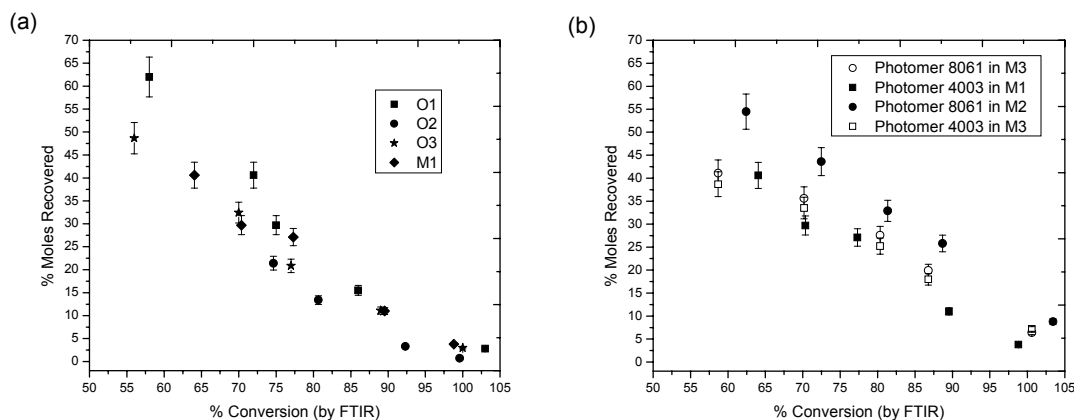
Figure 1. a. Photomer 4003 monomer recovery from film extracts. b. Monomer recovery from M series film extracts.

The molar amount of recovered Photomer 4003 at various conversion levels does not vary much for those samples in which it is the only co-monomer (Figure 1a). While the amount recovered from O1 at lower conversion levels is slightly higher than in the other samples, as curing proceeds the O1 recovery levels of Photomer 4003 become similar to those observed in the other samples. The exceptionally high level of monomer in O1 compared to the other samples may account for this observation. While the recovery of Photomer 4003 from O2 is similar to the other samples at higher conversion levels, it was not possible to obtain data for conversion levels less than 70%. In the M series, a slightly higher amount of the Photomer 8061 was recovered at all conversion levels in the M2 sample (where it is the sole co-monomer) compared to either monomer in the M1 or M3 samples (Figure 1b). This is consistent with the low conversion rate seen for M2. The Photomer 8061 and Photomer 4003 are consumed at similar rates when they are co-reactants in the M3 sample.

Gel permeation chromatography (GPC) was also used to evaluate molecular weight distributions (MWD) of the soluble, recovered oligomeric material for the various partially polymerized samples.

The shift of MWD of recovered material to higher values for all conversion levels in the O1 sample (Figure 2b) suggests the formation of soluble, high molecular weight material from Photomer 4003 homopolymerization, or the formation of material comprised of Photomer 4003 homopolymer fragments that have bonded to a urethane/acrylate oligomer before attachment to the growing, crosslinked network can take place. The technique does not allow us to distinguish between the two possibilities. The formation of this type of unbound material would be consistent with the suggestion that segregation of the Photomer 4003 molecules could be taking place to account for conversion rate differences, and would be more likely to take place in the O1 coating in which the amount of monomer relative to oligomer is so much greater than in the other formulations. While little change was seen in the MWD of recovered material for the O2 sample (not shown), it was shifted to lower values for all conversion levels of O3 (Figure 2c). This indicates the formation of low molecular weight oligomeric Photomer 4003 homopolymer which would also be consistent with segregation of the Photomer 4003 monomer.
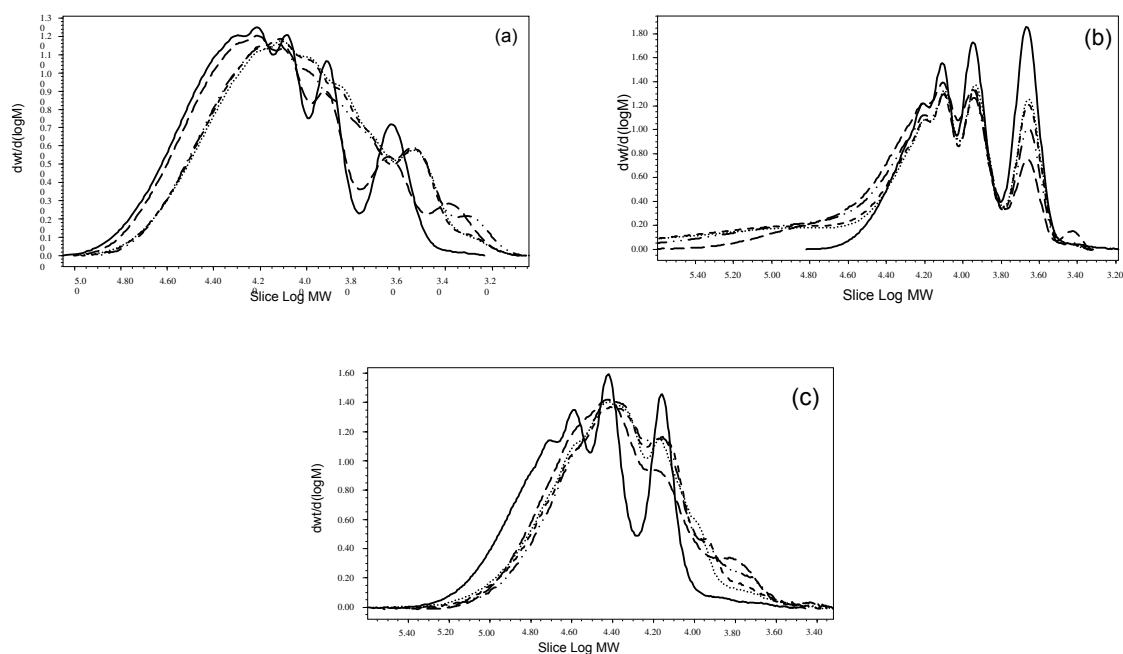
Figure 2. GPC MWD profiles of M2 (a), O1 (b) and O3 (c) formulation extracts. —— Oligomer standard, ········· extract from 60% cured film, ---- extract from 70% cured film, – ·· extract from 80% cured film, – – extract from 90% cured film.

The MWD of recovered oligomer resembled starting material for both M1 and M3 (not shown). In M2 a shift of recovered oligomer MWD to lower values is also seen at all conversion levels (Figure 2a). The unbound, oligomeric Photomer 8061 homopolymer that is extracted in M2 may be a consequence of slow monomer conversion rate coupled with a faster oligomer conversion rate – as indicated by the fairly short gel time resulting from a preference for oligomer reaction and network buildup in the early stages of the reaction. With oligomer tending to be depleted earlier, one might expect to see more oligomeric Photomer 8061 homopolymer in the 50 to 80% conversion range that has not had an opportunity to bind to the developing polymer network. For M1, unbound oligomeric Photomer 4003 homopolymer is not seen. At this point the Photomer 4003 homopolymer that was formed in the early part of the reaction as a result of monomer segregation, proposed to account for the

fast conversion rate, has had a chance to tie into the crosslinked polymer network. In contrast to M2, the gel time in M1 is greater because of the preference for monomer homopolymerization over oligomer reaction to build up the network in the early stages of the curing process.

The samples at intermediate conversion levels that were studied by extraction were also examined using solid state NMR ^{1}H T_2 relaxation measurements. The data in Figure 3 show a signal decay curve for one representative model film (M1) as a function of conversion level. Decay curves for the other samples had a similar qualitative appearance. As one increases the level of conversion in these systems, the ^{1}H NMR signal for the bulk polymer appears to decay at a faster rate, as evidenced by the steeper decay curves for samples with higher conversion levels. The simple qualitative analyses of these types of data demonstrate that such NMR measurements are very sensitive to differences in degree of conversion and can be useful in following the network development of polyurethane acrylate films.

The modified Kuhn formalism[12,16] allows us to adequately fit these ^{1}H T_2 data, as shown by the curves in Figure 3. This model contains two relaxation time constants, as well as prefactors related to the relative populations of the following: fully crosslinked chains, dangling chain ends and sol (unincorporated) material. These terms, which reflect the original modified Kuhn treatment terminology, may be somewhat overdescriptive and limiting. It may be more appropriate to simply describe populations of low, medium and high mobility. Each of these contributes to the shape of the ^{1}H T_2 decay curve and allows one to quantitatively treat these types of data. Populations of the low, medium and high mobility species are plotted for the O series of films as a function of degree of conversion in Figure 4. Similar plots were obtained for the M series but are not shown. The remaining parameters obtained by the fitting procedure are beyond the scope of this discussion.
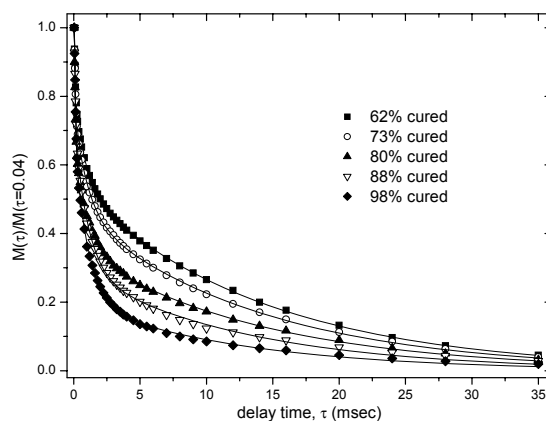
Figure 3. ^{1}H T_2 of partially cured solvent swollen M1 films. Solid lines represent fitting of data using the modified Kuhn expression described in the text.

Without exception, the sol fraction obtained from ^{1}H T_2 NMR data decreases with conversion level of the film. This is consistent with the idea that as the network develops during polymerization, the amount of highly mobile material decreases and eventually reaches a minimum value. For the fully polymerized films in these two series, the sol fraction is highest for the O3 film, most likely due to the highly mobile PPG8000 chain in the 1xPPG8000 oligomer used in this formulation. Even though bound into the network at both ends, a large portion of the polyol component of the oligomer may be quite mobile and appear as a sol-like structure, increasing the apparent amount of sol seen in O3 In general, the amount of "immobile" network material increases with degree of conversion, as one would have

expected. This includes the fraction of crosslinked chains, or network components possessing the least mobility, as well as the dangling chain component, representing material having an intermediate degree of mobility. In general, the rate of increase of the former with degree of conversion is less pronounced than the rate of increase of the latter or of the rate of decrease of sol component.
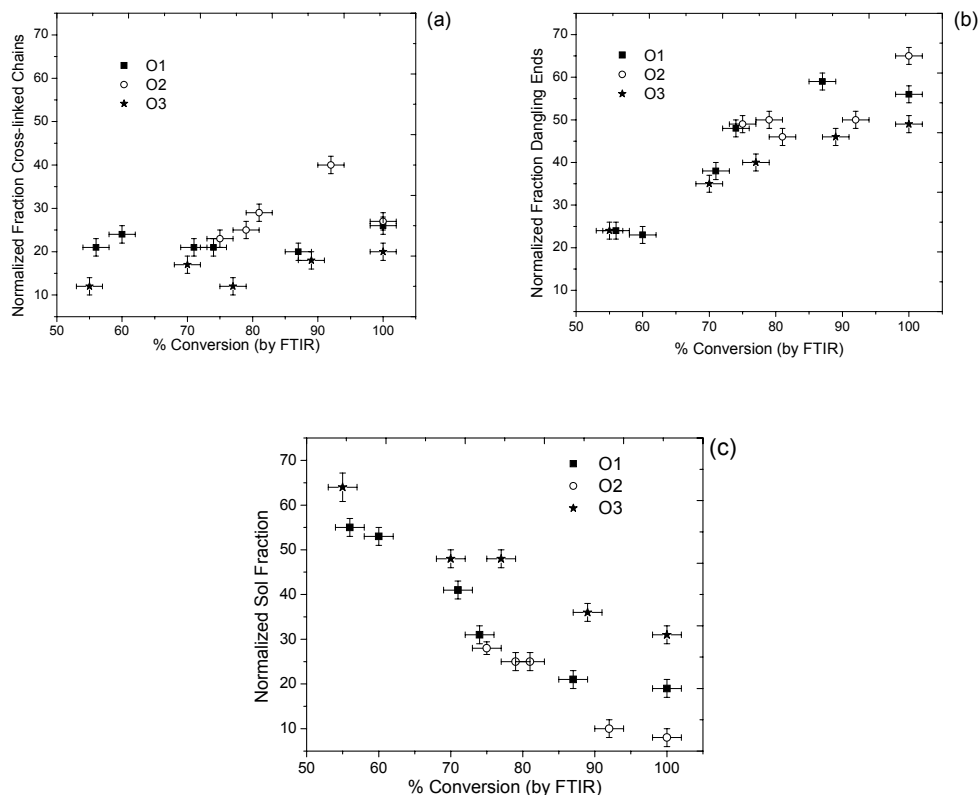
Figure 4. Normalized fractions of network chains in the O-series films as determined from ^{1}H T$_{2}$ NMR studies. (a) Fully crosslinked chains, (b) dangling ends and (c) sol fraction.

Comparing the decay curves for the fully polymerized films from each series is also instructive (Figure 5). The NMR decay curves obtained for the fully polymerized M series films (Figure 5b), demonstrate that these measurements are consistent for films having similar theoretical crosslink densities. The only difference in this series of films is the co-monomer used in the formulation, which has no direct effect on crosslinking. The steepest decay curve in Figure 5 belongs to the O2 film, which has the highest calculated, theoretical crosslink density in the O series (Table 1). Likewise, the other two O series films have lower crosslink densities and subsequently their ^{1}H T$_{2}$ decay curves are relatively less steep. The small difference between the O1 and O3 data in Figure 5a again illustrates the point made previously regarding the flexibility of the oligomer in O3. Since both samples should have identical crosslink densities, the slight difference in the curves must originate from differences in the dynamics of the oligomer polyol blocks. The fact that the curve for O1 decays slightly faster than O3 is consistent with the relative size and mobility differences of these oligomers.
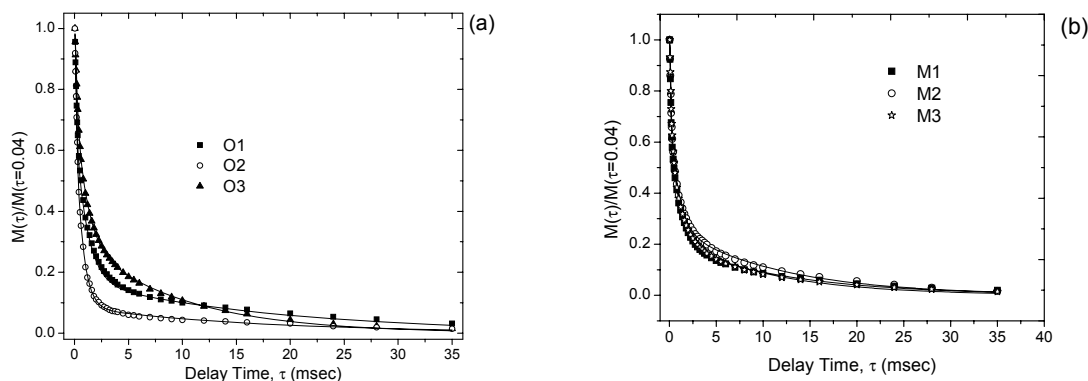
Figure 5. ^1H T_2 curves obtained for fully cured solvent swollen M and O series films. Solid lines denote fits to these data.

The relationship of the calculated crosslink density to polymer network properties can also be seen in the values of Young's modulus from stress-strain data for the fully converted polymer network films (Table 4). Young's modulus is expected to reflect the average molecular weight of elastically effective network chains between crosslinks, or M_c.[13] The values obtained do reflect the calculated crosslink levels given in Table 1, with the modulus values of O1 and O3 being roughly equal and less than the value for O2. The Young's modulus values for the M series were similar, and were between the values measured for the more heavily crosslinked O2 and the more lightly crosslinked O1 and O3 samples.

Table 4. Properties of fully cured samples.

	O1	**O2**	**O3**	**M1**	**M2**	**M3**
T_g ($^\circ$C)	-27	-26	-55 (sh), -37	-33	-44	-40
Young's modulus (MPa)	0.69±0.18	2.47±0.18	0.76±0.06	1.24±0.07	1.15±0.10	1.22±0.05

Also included in Table 4 are the glass transition temperatures for fully polymerized coating networks. The O3 sample is the only one that shows clear evidence in the DMA curve of phase separation between a polyol soft block and a diisocyanate/urethane and/or acrylic backbone hard block. These results are consistent with the fact that the separation between hard and soft domains in urethane based systems is expected to become more prevalent as the molecular weight of the polyol component increases.[17]

Conclusions

An integrated approach was taken to study polymer coating network development during photopolymerization for a series of fast reacting, low modulus coating formulations containing urethane/acrylate oligomers and acrylic co-monomers. For fully cured films, the trend in Young's modulus correlates well with the crosslink level based on size and amount of crosslinking oligomer. NMR relaxation studies on fully cured formulations agree with the Young's modulus trend once the high mobility of the oligomer polyol block is accounted for. Qualitatively, solid state NMR ^1H T_2 results showed a consistent correlation with cure level for all formulations. Analysis of extractables

showed formulation dependent differences in the rate of co-monomer incorporation and in the tendency to form additional, soluble oligomeric materials at intermediate cure levels. A combination of viscosity effects and structure dependent segregation of co-monomer could account for these observations. Kinetic photopolymerization experiments showed that the development of viscoelastic properties did not always increase with increasing monomer conversion rate. The observed conversion rates and gel times seem to be the result of a balance between initial viscosity and acrylate level that is unique for each formulation.

Acknowledgement

References

1. *Organic Coatings Science and Technology, Vols. 1 &2*; Wicks, Jr., Z. W., Jones, F. N., Pappas, S. P.; John Wiley & Sons, Inc.: New York, 1992.
2. Decker, C.; Moussa, K. *Makromol. Chem.* **1988**, *189*, 2381-2394.
3. Hoyle, C. E. In *Radiation Curing: Science and Technology*; Pappas, S. P., Ed.; Plenum: New York, **1992**.
4. Stansbury, J. W.; Dickens, S. H. *Polymer* **2001**, *42*, 6363-6369.
5. a. Lee, S. L.; Luciani, A.; Månson, J-A. E. *Prog. Org. Coatings* **2000**, *38*, 193-197; b. Steeman, P. A. M.; Dias, A.; Wienke, D.; Zwartkruis, T. *Macromolecules* **2004**, *37*, 7001-7007.
6. a. Fry, C. G.; Lind, A. C. *Macromolecules* **1988**, *21*, 1292-1297; b. Litvinov, V. M.; Dias, A. A. *Proceedings of the 50th IWCS*, **2001**, 267-272.
7. Decker, C.; Elzaouk, B.; Decker, D. *Pure Appl. Chem.* **1996**, *A33(2)*, 173-190.
8. Gasper, S.; Schissel, D.; Baker, L.; Smith, D.; Youngman, R.; Wu, L.; Sonner, S.; Givens, S.; Hancock, R. *Polym. Prepr. (Am. Chem. Soc., Div. Polym. Chem.)* **2003**, *44*, 27-28.
9. Youngman, R.; Schissel, D.; Gasper, S. *Polym. Prepr. (Am. Chem. Soc., Div. Polym. Chem.)* **2003**, *44*, 350-351.
10. a. Swiderski, K. W.; Khudyakov, I. V. *Ind. Chem. Eng. Res.*, **2004**, *43*, 6281-6284; b. Santhana, P.; Krishnan, G.; Choudhary, V.; Varma, I. K. *J. Macromol. Sci. Rev. Macromol. Chem. Phys.* **1993**, *C33(2)*, 147-180; c. McConnell J. A.; Willard F. K. In *ACS Symp. Ser., Radiation Curing of Polymeric Mateials)*; Hoyle, C. E., Kinstle, J. F., Eds.; **1990**, *417*, 272-283; d. Noren, G. K.; Zimmerman, J. M.; Krajewski, J. J.; Bishop, T. E. In *ACS Symp. Ser., Radiation Curing of Polymeric Mateials)*; Hoyle, C. E., Kinstle, J. F., Eds.; **1990**, *417*, 258-271.
11. Chambon, F.; Winter, H. H. *J. Rheol.* **1987**, *31*, 683-697.
12. Kuhn, W.; Barth, P.; Hafner, G.; Simon, G.; Schneider, H. *Macromolecules* **1994**, *27*, 5773-5779.
13. a. Kloosterboer, J. *Adv. Poly. Sci.* **1984**, *84*, 1-61; b. Dušek, K.; Dušková-Smr ková, M. *Prog. Poly. Sci.* **2000**, *25*, 1215-1260.
14. Lovell, L. G.; Stansbury, J. W.; Syrpes, D. C.; Bowman, C. N. *Macromolecules*, **1999**, *32*, 3913-3921.
15. Jansen, J. F. G. A.; Dias, A. A.; Dorschu, M.; Coussens, B. *Macromolecules*, **2003**, *36*, 3861-3873.
16. Borgia, G.C.; Fantazzini, A.; Ferrando, A.; Maddinelli, G. *Magn. Reson. Imaging* **2001**, *19*, 405-409.
17. Barbeau, Ph.; Gerard, J.F.; Magny, B.; Pascault, J.P.; Vigier, G. *J. Polym. Sci. B* **1999**, *37*, 919-937.